# ANEXOS I

En este apartado incluiré resultados, que a pesar de no haber sido incluidos en los manuscritos, ponen de manifiesto beneficios colaterales asociados a la administración de los nuevos donadores de NO específicos para plaquetas.

**ARTÍCULO SEGUNDO: *"A novel anti-ischemic nitric oxide donor inhibits thrombosis without modifying haemodynamic parameters".***

**OBJETIVO:** En este estudio, también determinamos el efecto de la administración oral de nitratos (IS-5-MN y LA419) en la expresión vascular de eNOS.

**MÉTODOS:** Tras la necroscopia, se obtuvo la porción proximal de la aorta torácica superior y cuidadosamente se diseccionó y separó la capa superior (contiene el endotelio) y la capa inferior (contiene la media) para analizarlas por separado. Una vez extraídas las muestras, se congelaron a -80ºC hasta su procesamiento. Para la extracción de proteína, las muestras se pulverizaron, homogeneizaron en tampón de lisis (50 mmols/L Tris-HCl, 1 mmols/L EDTA, 1% Triton X-100, 0.1 mg/mL PMSF, pH 7.4) y se cuantificaron mediante BCA (Pierce). Los niveles de eNOS se determinaron mediante la técnica de Western Blot. Así pues, las muestras de proteína (25 µg/carril) se corrieron mediante electroforesis en gel de acrilamida al 15% y seguidamente se transfirieron a una membrana de nitrocelulosa. Dicha membrana, primeramente se incubó con el anticuerpo primario (anticuerpo monoclonal anti-eNOS; Transduction Laboratories, UK) a una concentración de 1:2500 y posteriormente con anticuerpo secundario, a una concentración 1:10.000. La señal se reveló en un film radiográfico y la intensidad de las bandas obtenidas se cuantificó mediante un densitómetro.

**RESULTADOS**: ***(Anexo I - Figura 1)*** Al evaluar los resultados obtenidos, se observó -como era de esperar- que eNOS se expresa mayoritariamente en la capa endotelial. Igualmente, se observó (en la capa endotelial y en la capa media) una reducción significativa de la expresión proteínica de eNOS, en los animales a los que se les había administrado las dosis altas de LA419 (3.6-5 mg/Kg).

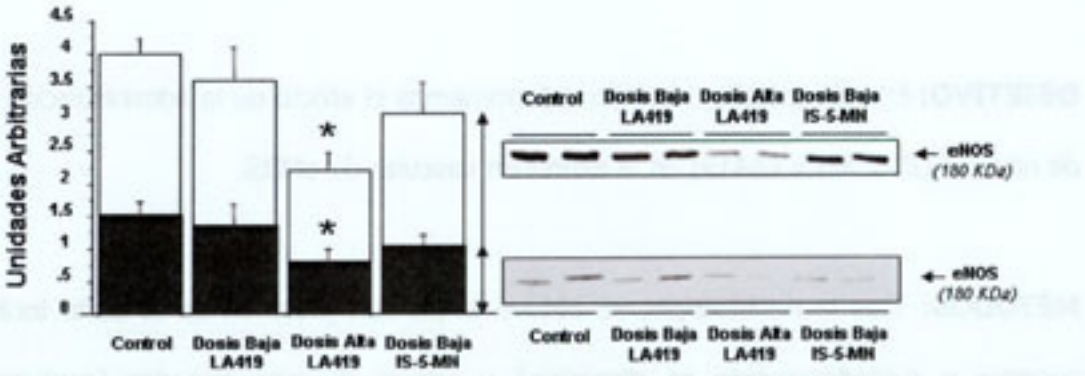


***Anexo I - Figura 1.*** Western Blot representativo de la expresión proteínica de eNOS en endotelio (barras blancas) y media (barras negras) de aorta torácica de todos los animales incluidos en el experimental. Las dosis bajas de donador de NO incluyen los animales tratados con 0.9 y 1.8 mg/Kg de LA419 o IS-5-MN, mientras las dosis altas incluyen los animales tratados con 3.6 y 5 mg/Kg de LA419.

**DISCUSIÓN:** Nuestros resultados están en línea con estudios anteriormente publicados, tanto *in vitro* (G. M Buga, y cols., 1993; Nosratola D.V, y cols., 1999) como *in vivo* (ratas) (Nosratola D.V, y cols., 1999), donde se describe la habilidad de los donadores de NO por disminuir su producción endógena, al disminuir la enzima responsable de su generación, la NO sintasa. A pesar de no conocerse con precisión el mecanismo que produce tal reducción, parece ser que ésta pretende normalizar la generación de nocivas especies reactivas de oxígeno, que se generarían por el exceso de NO. Por tanto, la reducción de eNOS en células vasculares, tras la administración de dosis altas de LA419, evitaría el exceso de NO y la consiguiente toxicidad celular.

Estos resultados también confirman que los efectos del LA419 no sólo se aprecian a nivel plaquetar, sino que también se aprecian a nivel de la pared vascular

# ANEXOS II
## (Otras Publicaciones)

ELSEVIER

Atherosclerosis 167 (2003) 55–63

ATHEROSCLEROSIS

www.elsevier.com/locate/atherosclerosis

# Differential intracellular trafficking of von Willebrand factor (vWF) and vWF propeptide in porcine endothelial cells lacking Weibel–Palade bodies and in human endothelial cells

Teresita Royo [1], José Martínez-González [1], Gemma Vilahur, Lina Badimon *

*Instituto de Investigación Cardiovascular de Barcelona, CSIC-ICCC-Hospital de la Santa Creu i Sant Pau, Arda. Sant Antoni Maria Claret # 167, Barcelona 08025, Spain*

Received 10 August 2002; received in revised form 14 October 2002; accepted 25 October 2002

**Abstract**

Von Willebrand factor (vWF) is an adhesive protein involved in primary haemostasis virtually absent in the thoracic aorta of swine, an animal model widely used in thrombosis and atherosclerosis. By RT-PCR analysis we show that porcine aortic endothelial cells (PAEC) express the vWF gene, although vWF mRNA levels were $8 \pm 0.8$-fold ($p < 0.05$) or $290 \pm 8.9$-fold ($p < 0.0001$) lower than those in porcine pulmonary artery EC (PPEC) or human aortic EC (HAEC), respectively. Although vWF was rare in the thoracic aorta of swine, vWF propeptide (vWFpp) was present in the endothelium of this artery and in both primary and passaged PAEC. In addition, vWFpp but not vWF was detected in PAEC by Western blot. In PAEC neither vWFpp nor P-selectin immunostaining depicted Weibel–Palade bodies (WPB)-like structures, and acute stimuli (α-thrombin or the calcium ionophore A23187) did not increase vWF secretion. vWFpp co-localized with a Golgi marker, that cycles between the stacked Golgi (SG fraction) and earlier compartments of the secretory pathway. Our results confirm that PAEC express very low levels of vWF mRNA and indicate that in these cells, that do not have WPB, vWF and vWFpp have divergent intracellular trafficking pathways.


*Keywords:* Endothelial cells; Von Willebrand factor; Golgi complex; Porcine model

## 1. Introduction

Von Willebrand factor (vWF) is a plasma glycoprotein that plays a central role in haemostasis. It is synthesized in megakaryocytes and endothelial cells (EC), and stored in platelet α-granules and in EC specialized secretory granules (Weibel–Palade bodies, WPB) that also contain the cell membrane protein P-selectin [1]. vWF is synthesized as a large precursor encompassing a signal peptide, a propeptide (vWFpp) and the mature protein. The precursor undergoes post-translational processing in the endoplasmic reticulum (ER) and in the Golgi and trans-Golgi network (TGN) [1]. After propeptide cleavage vWF follows either a constitutive secretory pathway or a regulated storage with the vWFpp (stoichiometry 1:1) in WPB [2]. The major part of endothelial vWF is slowly secreted through the constitutive pathway. By contrast, WPB constitute a fast release storage from which equimolar amounts of the largest, most biologically potent multimeric forms of vWF can be released after exocytosis-induced by stimulus such as thrombin generated by the coagulation cascade after tissue injury [1,3].

vWF mediates endothelial cell adhesion to the vessel wall, promotes platelet adhesion to the subendothelium in case of EC detachment, is essential for thrombus formation at high shear stress and acts as a chaperone/carrier protein for coagulation factor VIII [1]. Besides the well-established role of vWF in platelet adhesion and thrombosis [4–6], vWF could also play a role in atherogenesis, although its involvement in atherosclerotic lesion development is less clear [7–10].

The porcine vascular tree exhibits a heterogeneous distribution of WPB and vWF, in fact both WPB and

* Corresponding author. Tel./fax: +34-93-291-9285.
*E-mail address:* lbmucv@cid.csic.es (L. Badimon).
[1] Both authors contributed equally to this work.

0021-9150/02/$ - see front matter 
PII: S0021-9150(02)00393-3

vWF are virtually absent in porcine thoracic aorta [11–14]. Although early analysis by slot blot using heterologous probes suggested the presence of the vWF transcript in porcine thoracic aorta EC (PAEC) [15], it has not been documented by more specific molecular biology techniques; on the other hand, in these cells the processing of vWF/vWFpp has not been addressed. The present study was designed to ascertain vWF mRNA levels in PAEC and to assess whether these cells synthesize and process vWF. We show that PAEC exhibit low vWF mRNA and protein levels, but significant vWFpp immunolabeling indicating a divergent fate of vWFpp once cleaved of vWF. vWFpp was non-associated to WPB but co-localized with formiminotransferase cyclodeaminase (FTCD), a protein that cycles between the stacked Golgi (SG fraction) and earlier compartments of the secretory pathway.

## 2. Methods

### 2.1. Materials

Cultured media and reagents were from GibcoBRL (Renfrewshire, UK). Polyclonal antibody specific for porcine vWFpp (*pabBp19*) was prepared as previously described [16,17]. Polyclonal antibody against human vWFpp (Frieda 013091) was a gift from Dr Kroner and Dr Montgomery (the Blood Center of Southeastern Wisconsin, Milwaukee, USA). Polyclonal antibodies anti-vWF (A-0082; Dako, Glostrup, Denmark) and anti-P-selectin (09361A; Pharmingen Europe, Spain), that recognize both human and porcine proteins were used [17,18]. Monoclonal antibodies anti-endothelial nitric oxide synthase (eNOS, clone 3; Transduction Laboratories, Lexington, KY, USA) and anti-FTCD (clone 58-9; Sigma, St. Louis, MO, USA) [19], were used for co-location experiments. Thrombin was from Diagnostica Stago (Asnières, France). Other materials and chemicals were from Sigma unless otherwise stated.

The procedures performed in this study were all in accordance with appropriate institutional guidelines and also followed the *Guide for the Care and Use of Laboratory Animals* published by the US National Institutes of Health (NIH Publication No. 85-23, revised 1985). Human aortas used for cell isolation were taken from donated corpses (Hospital Vall d'Hebrón, Barcelona, Spain) following the guidelines of the Committee of Human Research.

### 2.2. Immunohistochemistry from porcine arteries

Porcine arteries (from Yorkshire-Albino pigs, 35±5 kg) were processed and consecutive sections were prepared as described [20]. Double indirect immunofluorescence was carried out using one polyclonal antibody [*pabBp19* (1:200) or anti-vWF (1:100)] and one monoclonal antibody (anti-eNOS, 1:200). Primary antibodies were diluted in 100 mM PBS/200 mM glycine/0.1% Triton X-100/1% BSA. Oregon Green® 488 goat anti-rabbit IgG and Texas Red®-X goat anti-mouse IgG (1:100; Molecular Probes, Europe BV, Leiden, The Netherlands) were used as secondary antibodies. Labeled sections were mounted in Mowiol® 4-88 (Calbiochem, La Jolla, CA, USA) and analyzed by confocal microscopy in a Leica TCS 4D system (Heidelberg, Germany). Controls incubated with non-immune rabbit γ-globulin and without the primary antibody were included in all the procedures.

### 2.3. Cell culture

PAEC and EC from porcine pulmonary artery (PPEC) and human thoracic aorta (HAEC) were obtained by collagenase digestion as described previously [21]. EC were cultured in medium 199 supplemented with 25 mM Hepes, 2 mM L-glutamine, 50 U/ml penicillin, 0.05 mg/ml streptomycin and 10% heat-treated fetal calf serum (FCS) (Biological Industries, Haemek, Israel). Since vWF biosynthesis decrease with cell passaging and the enzymatic treatment could activate the release of stored vWF we analyzed vWpp/vWF in porcine non-passaged EC (unless otherwise stated).

### 2.4. Northern blot analysis

Total RNA from EC (2nd passage) was isolated using Ultraspec™ (Biotecx, Houston, TX, USA). Total RNA was fractionated in 1% agarose gels containing formaldehyde, was transferred by capillarity to Hybond-N™ (Amersham-Pharmacia, Buckinghamshire, UK) membranes and UV-crosslinked. Human and porcine vWF cDNAs were synthesized by PCR (see below), purified from agarose-ethidium bromide gels by Geneclean™ kit (Bio 101 Inc.), labelled with [α-$^{32}$P]dCTP (3000 Ci/mmol, Amersham-Pharmacia) by Random Primed DNA labeling kit (Roche, Mannheim, Germany) and used as probes. Filters were prehybridized and hybridized as described previously [21].

Human and porcine vWF cDNAs were synthesized by PCR. Total RNA was reverse transcribed and an aliquot of cDNA obtained was amplified in a reaction mixture containing: 0.2 mM of each dNTP, 1 U Expand™ High Fidelity DNA polimerase (Roche) and 100 ng of each specific oligonucleotide in 1 × Buffer and 1.5 mM $MgCl_2$ as described [21]. The specific oligonucleotides were: human vWF, 5′-tct ggc tga ggg agg taa aa-3′ and 5′-ggc att gag aac ctc atg gt-3′, positions 8413 and 8713, respectively, within the human cDNA (Accession No. NM000552); porcine vWF, 5′-gga ggc ctg tct act caa cg-3′ and 5′-tga ccc tgc aga agt gac tg-3′,

positions 6745 and 7043, respectively, within the porcine cDNA (Accession No. AF052036). Levels of glyceraldehyde-3-phosphate deshidrogenase (GAPDH) were used to normalize results [21]. Amplification was carried out: 94 °C 30 s, 61 °C 1 min and 72 °C 1 min (vWF, 35 cycles; GAPDH 30 cycles) followed by a final extension of 72 °C 5 min. DNA sequencing of PCR products, using the ABIPrism™Bigdye terminator cycle sequencing kit (Perkin–Elmer, Foster City, CA, USA), confirmed vWF identity.

### 2.5. RT-PCR analysis labeling PCR products with digoxigenin

vWF expression was comparatively analyzed in human and porcine EC by RT-PCR using a highly sensitive detection method that label PCR products with digoxigenin [21]. Since vWF mRNA levels in the EC analyzed were quite different the amount of cDNA from each cell type used as template in PCR reactions was adjusted as follows PAEC/PPEC/HAEC: 1/5/250. In these conditions vWF mRNA levels were analyzed after 27 cycles (within the exponential amplification phase). Briefly, PCR products were electrophorezed, transferred onto nylon membranes and UV-crosslinked. Detection of digoxigenin-labeled nucleic acids was performed with an anti-digoxigenin antibody linked to alkalyne phosphatase using CSPD as substrate. Filters were exposed to X-ray films and relative amounts of RNA were measured by densitometric scanning.

### 2.6. Protein extracts and Western blot analysis

Cellular supernatants were collected and stored at −70 °C. Cell monolayers were washed twice in DPBS, scrapped in lysis buffer (50 mM Tris–HCl, 1 mM EDTA, 1% Triton X-100, 0.1 mg/ml PMSF, pH 7.4) and, after sonication and centrifugation, were stored at −70 °C. Protein was quantified by the bicinchoninic acid (BCA) method using the BCA Protein Assay Reagent™ (Pierce, Rockford, IL, USA). Total protein (40 μg) were run in 7.5% PAGE and levels of vWFpp and vWF were analyzed by Western blot as described [17].

### 2.7. Immunocytochemistry from cultured EC

Primary EC and passaged EC (first passage) were processed for immunocytochemistry as described [16]. After blocking, cells were incubated with the primary antibody [*pabBp19* (1:100); anti-vWF (1:100); anti-P-selectin (1:250) or anti-FTCD (1:25)] at 37 °C for 1 h. Fluorescein (FITC) goat anti-rabbit IgG conjugate (1:100; Sigma) and rhodamine (TRITC) goat anti-mouse IgG conjugate (1:200; Sigma) were used as secondary antibodies. Samples and controls were mounted and analyzed as indicated above.

### 2.8. Brefeldin A experiments

Porcine EC were treated with brefeldin A (1 μg/ml) for 15, 30 and 60 min. Cells were then washed twice with DPBS at 37 °C, fixed with DPBS/4% paraformaldehyde/30% sucrose 10 min at room temperature and washed twice with DPBS. Immunocytochemistry was performed as described above.

### 2.9. Secretion studies and vWF determinations

Confluent monolayers of EC grown in 24-well plates were washed three times and preincubated in 1 ml Krebs–Ringer-bicarbonate buffer (KRBH) for 10 min at 37 °C. After a fourth wash, cells were incubated in 0.3 ml KRBH with either thrombin (1 U/ml) or the calcium ionophore A23187 (10 μM) for 30 min. The cell supernatants were centrifuged and kept at −20 °C until determination of vWF by ELISA as described [17]. Results are shown as means ± S.E.M. of three experiments performed in duplicate. Data are expressed as percentages relative to control values (the release by unstimulated cells after 30 min). The significance of differences was calculated using the student *t* test.

## 3. Results

### 3.1. Immunolabeling of vWFpp and vWF in porcine arteries

In agreement with previous results, vWF immunolabeling was rare in the porcine thoracic aorta. Immunostaining with eNOS, a non-secreted endothelial protein, showed a weak co-localization pattern (Fig. 1A and C). A different feature was seen in porcine pulmonary artery that clearly exhibited vWF immunolabeling in the endothelium (co-localizing with eNOS) and in the subendothelium nearest the lumen (Fig. 1B and D). However, we evidenced that vWFpp immunolabeling was present in the endothelium of serial sections of the pig thoracic aorta as well as in the pulmonary artery, and in both cases strictly co-localized with eNOS (Fig. 1E–H).

### 3.2. vWF expression in porcine EC

vWF expression in porcine and human EC was analyzed by Northern blot using as probes homologous cDNAs corresponding to either the human or porcine vWF gene. As Fig. 2A shows, this technique detected high vWF mRNA levels in HAEC, whereas in porcine

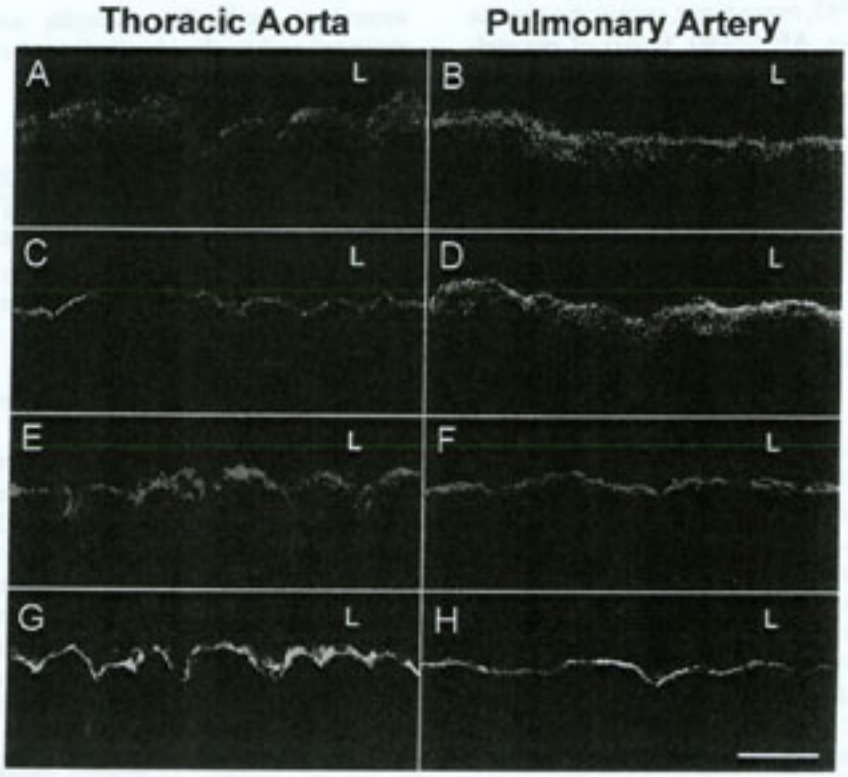


Fig. 1. vWF and vWFpp in porcine arteries. A–D, immunolabeling with anti-vWF (green) alone (A, B) or in combination with eNOS (red) (C, D). E–H, immunolabeling with anti-vWFpp (*pabBP19*, green) alone (E, F) or in combination with eNOS (red) (G, H). Bar: 25 μm. L, lumen.

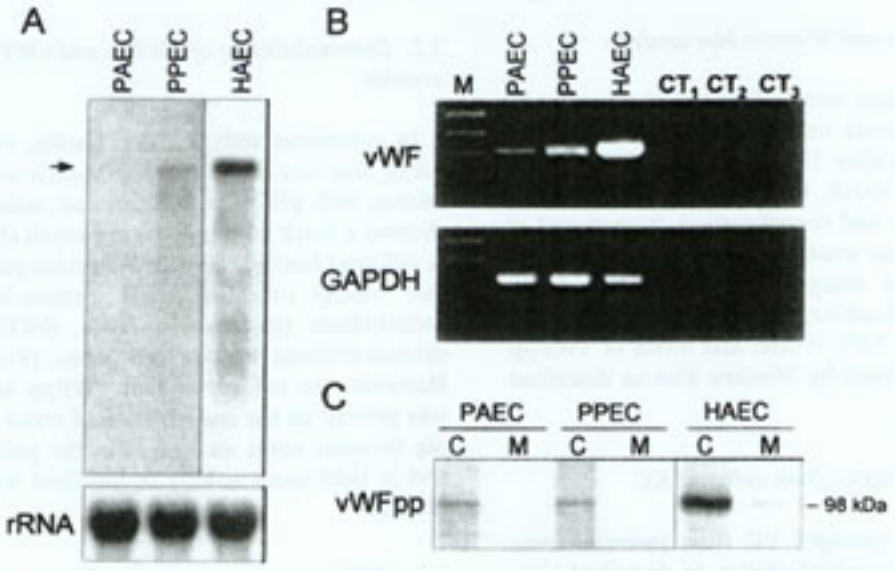


Fig. 2. vWF expression in EC. A, Northen blot from total EC RNA (10 μg per lane) hybridized with homologous probe (porcine or human vWF cDNAs) corresponding to the C-terminus of vWF. The position of the approximately 8.9 kb vWF mRNA identified in HAEC and PPEC is indicated. Filter was hybridized with 28S ribosomal RNA (rRNA) as a loading control. B, Ethidium bromide staining of PCR products corresponding to vWF or GAPDH from PAEC, PPEC and HAEC. vWF cDNA were amplified using specific primers for either porcine or human vWF cDNA sequences as indicated in Methods. CT-1, -2 and -3 (Controls, non-retrotranscribed RNA) from PAEC, PPEC and HAEC amplified with either vWF or GAPDH primers. M corresponds to molecular size markers. C, vWFpp levels in cell extracts (C) and cell media (M) from human (HAEC) and porcine EC (PAEC, PPEC). Porcine and human vWFpp were identified using the corresponding specific antibodies (*pabBP19* or Frieda 013091, respectively).

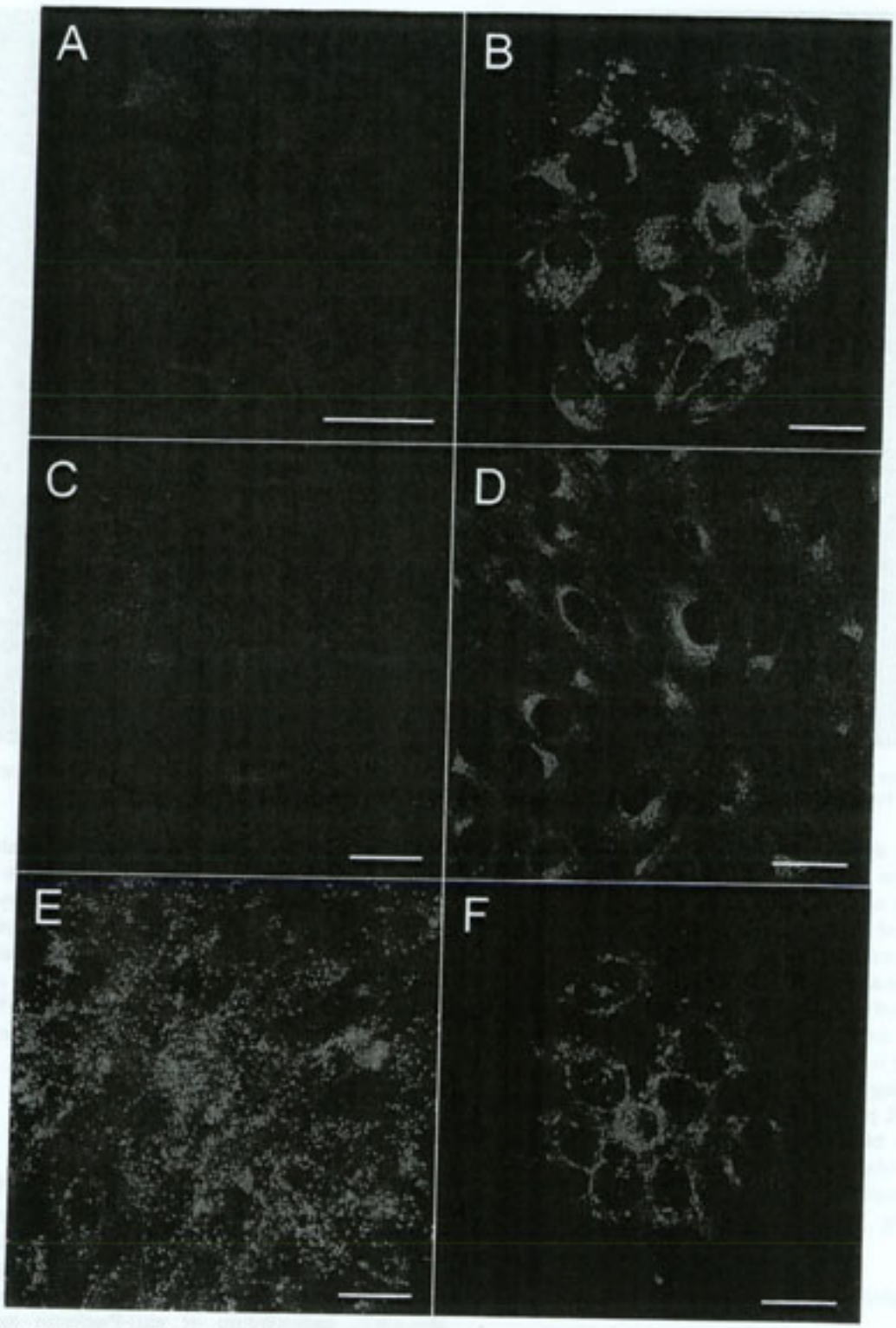


Fig. 3. vWF and vWFpp in porcine EC. Porcine EC from thoracic aorta (PAEC; A–D) and pulmonary artery (PPEC; E and F) were immunolabeled using anti-vWF antibodies (A, C and E) or anti-vWFpp antibodies (*pabBp19*; B, D and F). Immunostaining showed in A, B, E and F correspond to cells analyzed 18 h after isolation from the corresponding arteries. Bars: 10 μm.

EC samples vWF mRNA was weakly detected in PPEC after over-exposition of the films.

Detection of vWF mRNA in PAEC required amplification by RT-PCR. After PCR amplification, vWF

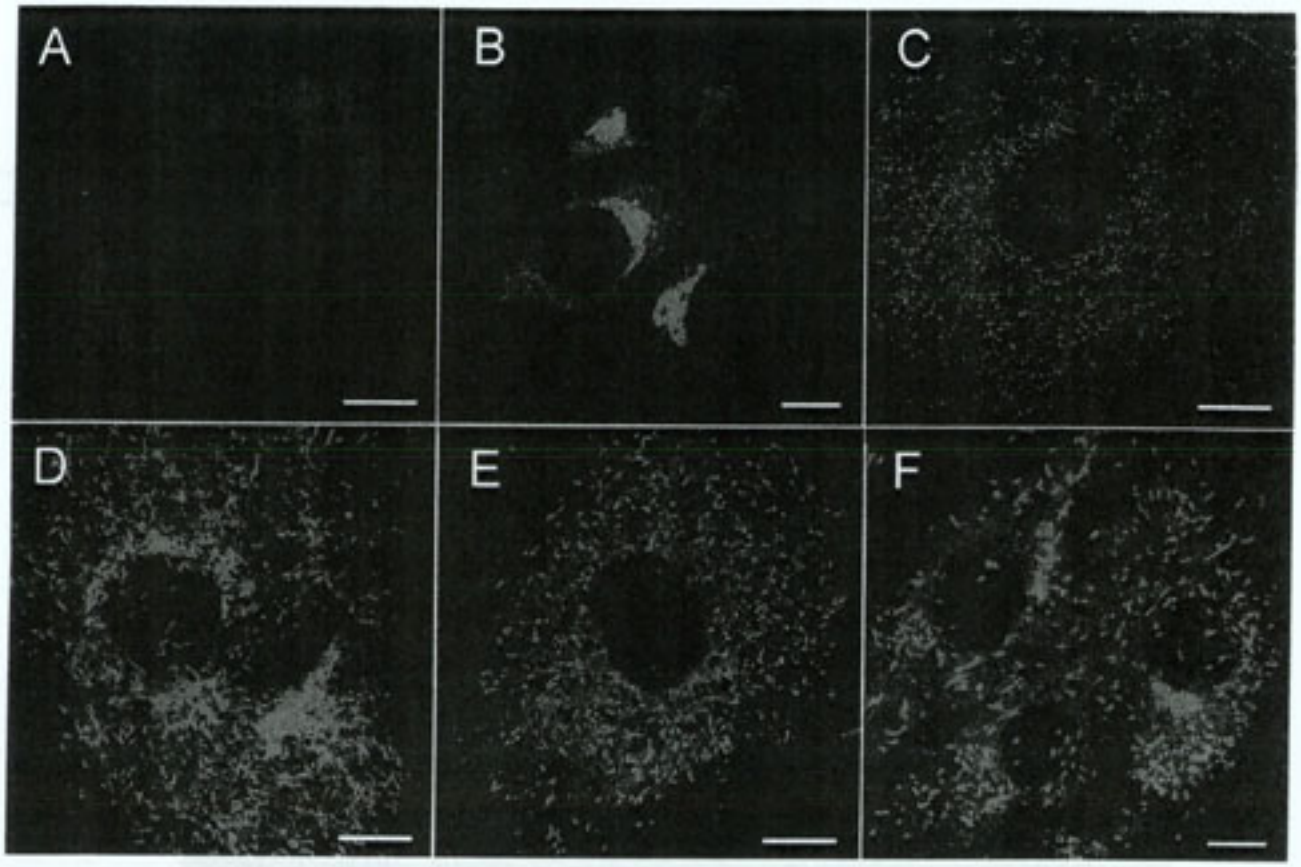


Fig. 4. Comparison of immunostaining patterns in PAEC (A–C) and HAEC (D–F). Immunostaining corresponds to vWF (A and D), vWFpp [with *pabBp19* (B) and Frieda 013091 (E)] and P-selectin (C and F). Bars: 5 μm.

cDNAs were amplified from both porcine EC and HAEC samples (Fig. 2B). As shown in this figure, no PCR products were observed in negative controls (non-retrotranscribed RNA), and similar results were obtained from samples treated with DNAse free RNAse (data not shown). RT-PCR analysis from different cell batches revealed that vWF mRNA levels in PAEC were lower than in either HAEC ($290 \pm 8.9$-fold, $p = 0.0001$) or PPEC ($8 \pm 0.5$-fold, $p < 0.05$). These results were confirmed using a highly sensitive detection method that label PCR products with digoxigenin.

By Western blot vWF protein levels in PAEC were undetectable (data not shown), but vWFpp protein levels were detectable in cell extracts from both PAEC and PPEC (Fig. 2C).

### 3.3. Immunolabeling of vWFpp and vWF in cultured EC

In agreement with Northern blot and Western blot experiments, vWF was not detected by immunocytochemistry in PAEC even in cells analyzed 18 h after isolation (Fig. 3A and C). In contrast, anti-vWFpp antibodies specifically immunolabeled the perinuclear area of PAEC in both primary and passaged cultures (Fig. 3B and D). This immunolabeling was abrogated when antibodies were previously incubated with purified porcine vWFpp (data not shown). Primary PPEC cultures showed significant staining for both vWF (Fig. 3E) and vWFpp (Fig. 3F). In these cells vWF immunostaining yielded granular staining and the typical irregular 'patches' corresponding to vWF that remain associated to cells or trapped underneath cell monolayer [22].

### 3.4. Subcellular localization vWFpp in PAEC

Neither vWFpp (Fig. 4B) nor P-selectin (Fig. 4C) immunolabeling depicted the typical pattern corresponding to WPB-like structures (elongated/rob-shaped structures scattered throughout the cytoplasm) in PAEC. In contrast, HAEC showed this pattern with anti-vWF, anti-vWFpp or anti-P-selectin antibodies (Fig. 4D–F). Electron microscopy confirmed that PAEC did not posses WPB (data not shown), as previously described in thoracic aorta endothelium [14]. Finally, neither thrombin (1 U/ml) nor the calcium ionophore A23187 (10 μM) produced significant release of vWF ($103 \pm 7$ and $98 \pm 5\%$, respectively) from PAEC

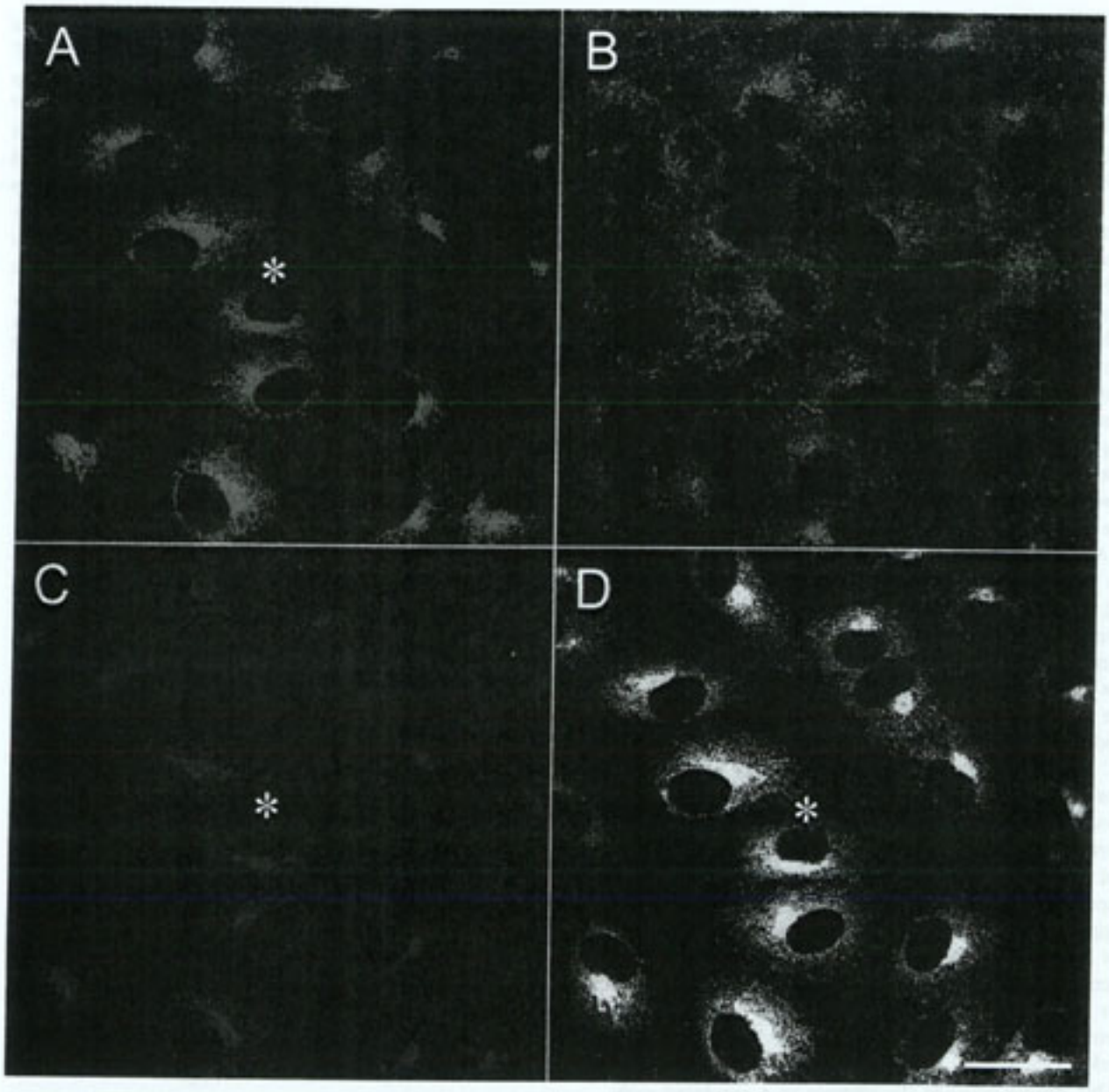


Fig. 5. Subcellular location of porcine vWFpp in the Golgi complex. vWFpp staining of PAEC without any treatment (A) or after 15 min of brefeldin A treatment (B). Immunolabeling with anti-FTCD antibody (*red*) alone (C) or in combination with anti-vWFpp antibodies (*pabBp19*; co-localization yellow) (D). Bar: 20 μm. *, Indicates a cell under different conditions.

after 30 min of stimulation (similar results were obtained after longer stimulation periods), confirming previous observations by Giddings et al. indicating that vWF is not significantly accumulated in PAEC with time [11]. In contrast, both thrombin and the calcium ionophore A23187 significantly induced vWF release from HAEC [310 ± 47 and 230 ± 53%, respectively ($P < 0.05$), after 30 min].

Treatment of PAEC with brefeldin A, a compound that disorganizes the Golgi complex, dislocalized vWFpp immunolabeling (Fig. 5B). Co-localization analysis with FTCD, a protein that cycles between the stacked Golgi (SG fraction) and earlier compartments of the secretory pathway [19], shows that vWFpp is localized in the Golgi complex (Fig. 5A, C and D).

## 4. Discussion

We and others have observed heterogeneity in vWF expression in the endothelium of porcine arteries, that in contrast to humans and other animal models, are

negative or only 'weakly' positive for vWF in the thoracic aorta [11–15]. The 'virtual absence' of vWF in the endothelium of porcine thoracic aorta was early correlated with the resistance to spontaneous atherosclerosis in this vascular bed [7–9], an observation supported by recent findings showing a localized reduction of atherosclerosis in areas prone to develop lesions in vWF-deficient mice [23]. A differential local regulation of key molecules involved in vascular cell functions could be the reason for the observed regionalization in atherosclerosis and thrombosis. Since the pig is an animal model widely used in thrombosis and atherosclerosis [24], our interest was to analyze the expression and synthesis of vWF in PAEC, cells that virtually do not have WPB. The present results confirm that PAEC presents low vWF levels as a result of their low vWF expression, and show for the first time that in these cells, that do not store vWF, vWF and vWFpp trafficking diverge leading to an apparent 'retention' of vWFpp in the Golgi.

Although vWF was rare in the porcine thoracic aorta we detected significant levels of vWFpp. vWFpp labeling pattern was similar in thoracic aorta and pulmonary artery; in both arteries it was restricted to the endothelium. By contrast, vWF staining was clearly identified in the pulmonary artery, in both the endothelium and in the subendothelium, probably as a result of its high avidity to extracellular matrix proteins once secreted by EC [25], an avidity that is not shared by vWFpp [22]. The production of vWF by EC from thoracic aorta was also examined in PAEC cultures. RT-PCR analysis shown that vWF mRNA levels in PAEC were about 8 and 290-fold lower than those of PPEC and HAEC, respectively. These data confirm previous observations suggesting that a low vWF expression determines the low vWF synthesis in these cells. However, in concordance with the observations in intact arteries, vWFpp was clearly detected in PAEC by both immunocytochemistry and Western blot, although no detectable levels of vWF were found by these techniques.

Our results confirm the absence of a regulated pathway of secretion in PAEC, as indicated by the absence of WPB structures that were not detected either by immunostaining or by electron microscopy analysis, and the inability of stimuli to acutely induce vWF secretion. WPB are secretory specialized organelles that in other mammalian species including humans store a myriad of molecules involved in atherogenesis, besides vWF and P-selectin, factor VIII, t-PA, interleukine-8 and endothelin-1 [26,27]. Since these molecules are local mediators involved in thrombosis and atherosclerosis, the lack of a regulated pathway of secretion in the endothelium of the thoracic aorta could impair these processes, beyond the relative deficiency of vWF.

The biosynthesis and complex post-translational processing of the vWF precursor in the Golgi and TGN have focused the interest of different investigators in the last years. The propeptide seems to be required for vWF trafficking to storage granules [2,28,29]; in fact, vWFpp also traffics an unrelated protein to storage [30]. vWF most likely continues associated with vWFpp in the TGN, and both proteins are subsequently cotransported to storage by virtue of the sorting signal on vWFpp remaining non-covalently associated with vWF (1:1 stoichiometric ratio) in the WPB [22,29]. In porcine thoracic aorta EC, that seem to be devoided of WPB, we observed that vWFpp is mainly located in the Golgi, since it co-localizes with a Golgi marker that cycles between the SG fraction and earlier compartments of the secretory pathway. The analysis of the porcine vWFpp amino acid sequence, which N-terminus we reported for the first time [17], and which full-length sequence has been recently communicated by Fahs et al. (Accession No. AY0044876), did not reveal any clue about the divergent fates of vWF and vWFpp in PAEC. The mechanism by which proteins are sorted to storage granules is not well defined. A hypothesis proposes that the targeting sequence(s) on the stored protein interacts with specific receptor(s) to initiate storage. Further experiments focused on differential gene expression analysis in PAEC could clarify whether the particular trafficking of vWFpp/vWF in these cells, that not seems to be shared by EC from other porcine vascular beds, could be associated to the expression of this putative receptor(s).

## Acknowledgements

This work was supported in part by grants Marató TV3-Malalties Cardíaques/96-10, FIS 98/0715, FIS 99/0907, SAF 2000/0174 and Fundación de Investigación Cardiovascular (FIC)-Catalana Occidente. We would like to give special thanks to Dr Kroner and Dr Montgomery for providing the polyclonal antibody Frieda 013091 against human vWFpp.

## References

[1] Wagner DD. Cell biology of von Willebrand factor. Annu Rev Cell Biol 1990;6:217–46.
[2] Wagner DD, Saffaripour S, Bonfanti R, Sadler JE, Cramer EM, Chapman B, Mayadas TN. Induction of specific storage organelles by von Willebrand factor propolypeptide. Cell 1991;64:403–13.
[3] Sporn LA, Marder VJ, Wagner DD. Inducible secretion of large, biologically potent von Willebrand factor multimers. Cell 1986;46:185–90.
[4] Turitto VT, Weiss HJ, Zimmerman TS, Sussman II. Factor VII/von Willebrand in subendothelium mediantes platelet adhesion. Blood 1985;65:823–31.
[5] Nichols TC, Bellinger DA, Reddick RL, Read MS, Koch GG, Brinkhous KM, Griggs TR. Role of von Willebrand factor in

arterial thrombosis. Studies in normal and von Willebrand disease pigs. Circulation 1991;83:IV56–64.
[6] Nichols TC, Samama CM, Bellinger DA, et al. Function of von Willebrand factor after crossed bone marrow transplantation between normal and von Willebrand disease pigs: effect on arterial thrombosis in chimeras. Proc Natl Acad Sci USA 1995;92:2455–9.
[7] Fuster V, Bowie EJW, Lewis JC, Fass DN, Owen CA, Jr, Brown AL. Resistance to arteriosclerosis in pigs with von Willebrand's disease. Spontaneous and high cholesterol diet-induced arteriosclerosis. J Clin Invest 1978;61:722–30.
[8] Griggs TR, Reddick RL, Sultzer D, Brinkhous KM. Susceptibility to atherosclerosis in aortas and coronary arteries of swine with von Willebrand's disease. Am J Pathol 1981;102:137–45.
[9] Badimon L, Steele P, Badimon JJ, Bowie EJW, Fuster V. Aortic atherosclerosis in pigs with heterozygous von Willebrand disease. Comparison with homozygous von Willebrand and normal pigs. Arteriosclerosis 1985;5:366–70.
[10] Nichols TC, Bellinger DA, Reddick RL, et al. von Willebrand factor does not influence atherosclerosis in arteries subjected to altered shear stress. Arterioscler Thromb Vasc Biol 1998;19:323–30.
[11] Giddings JC, Jarvis AL, Bloom AL. Differential localization and synthesis of porcine factor VIII related antigen (VIIIR:Ag) in vascular endothelium and in endothelial cells in culture. Thromb Res 1983;29:299–312.
[12] Wu QY, Drouet L, Carrier JL, et al. Differential distribution of von Willebrand factor in endothelial cells: comparison between normal pigs and pigs with von Willebrand disease. Arteriosclerosis 1987;7:47–54.
[13] Rand JH, Badimon L, Gordon RE, Uson RR, Fuster V. Distribution of von Willebrand factor in porcine intima varies with blood vessel type and location. Arteriosclerosis 1987;7:287–91.
[14] Gebrane-Younès J, Drouet L, Caen JP, Orcel L. Heterogeneous distribution of Weibel–Palade bodies and von Willebrand factor along the porcine vascular tree. Am J Pathol 1991;139:1471–84.
[15] Bahnak BR, Wu QY, Coulombel L, et al. Expression of von Willebrand factor in porcine vessels: Heterogeneity at the level of von Willebrand factor mRNA. J Cell Physiol 1989;138:305–10.
[16] Royo T, Vidal M, Badimon L. Purification of the porcine platelet GP IIb-IIIa complex and the propolypeptide of von Willebrand factor. Thromb Haemost 1998;80:302–9.
[17] Royo T, Vidal M, Badimon L. Porcine platelet von Willebrand Antigen II (vW AgII): Inhibitory effect on collagen induced aggregation and comparative distribution with human platelets. Thromb Haemost 1998;80:677–85.
[18] Chen D, Riesbeck K, McVey JH, Kemball-Cook G, Tuddenham EG, Lechler RI, Dorling A. Regulated inhibition of coagulation by porcine endothelial cells expression P-selectin-tagged hirudin and tissue factor pathway inhibitor fusion proteins. Transplantation 1999;68:832–9.
[19] Gao YS, Alvarez C, Nelson DS, Sztul E. Molecular cloning, characterization, and dynamics of rat formiminotransferase cyclodeaminase, a golgi-associated 58-kDa protein. J Biol Chem 1998;273:33825–34.
[20] Royo T, Alfón J, Berrozpe M, Badimon L. Effect of gemfibrozil on peripheral atherosclerosis and platelet activation in a pig model of hyperlipidemia. Eur J Clin Invest 2000;30:843–52.
[21] Martínez-González J, Raposo B, Rodríguez C, Badimon L. 3-hydroxy-3-methylglutaryl coenzyme A reductase inhibition prevents endothelial NO synthase downregulation by atherogenic levels of native LDLs. Arterioscler Thromb Vasc Biol 2001;21:804–9.
[22] Wagner DD, Fay PJ, Sporn LA, Sinha S, Lawrence SO, Marder VJ. Divergent fates of von Willebrand factor and its propolypeptide (von Willebrand antigen II) after secretion from endothelial cells. Proc Natl Acad Sci USA 1987;84:1955–9.
[23] Methia N, Andre P, Denis CV, Economopoulos M, Wagner DD. Localized reduction of atheosclerosis in von Willebrand factor-deficient mice. Blood 2001;98:1424–8.
[24] Badimon L. Atherosclerosis and thrombosis: lessons from animal models. Thromb Haemost 2001;86:356–65.
[25] Sporn LA, Marder VJ, Wagner DD. von Willebrand factor released from Weibel–Palade bodies binds more avidly to extracellular matrix than that secreted constitutively. Blood 1987;69:1531–4.
[26] Rosenberg JB, Foster PA, Kaufman RJ, Vokac EA, Moussali M, Kroner PA, Montgomery RR. Intracellular trafficking of factor VIII to von Willebrand factor storage granules. J Clin Invest 1998;101:613–24.
[27] Rosnoblet C, Vischer UM, Gerard RD, Irminger JC, Halban PA, Kruithof EKO. Storage of tissue-type plasminogen activator in Weibel–Palade bodies of human endothelial cells. Arterioscler Thromb Vasc Biol 1999;19:1796–803.
[28] Haberichter SL, Fahs SA, Montgomery RR. Von Willebrand factor storage and multimerization:2 independent intracellular processes. Blood 2000;96:1808–15.
[29] Van Mourik JA, Romani de Wit T. Von Willebrand factor propeptide in vascular disorders. Thromb Haemost 2001;86:164–71.
[30] Haberichter SL, Jozwiak MA, Rosenberg JB, Christopherson PA, Montgomery RR. The von Willebrand factor propeptide (vWFpp) traffics an unrelated protein to storage. Arterioscler Thromb Vasc Biol 2002;22:921–6.

ELSEVIER

Cardiovascular Research 58 (2003) 178–185

Cardiovascular Research

www.elsevier.com/locate/cardiores

# Modulation of ERG25 expression by LDL in vascular cells

C. Rodriguez, B. Raposo, J. Martínez-González, V. Llorente-Cortés, G. Vilahur, L. Badimon*

*Cardiovascular Research Center, ICCC-CSIC, Hospital de la Santa Creu i Sant Pau, Avda. St. Antoni Maria Claret 167, 08025 Barcelona, Spain*

Received 21 October 2002; accepted 9 December 2002

**Abstract**

**Background:** Plasma low density lipoproteins (LDL) play a key role in the pathogenesis of atherosclerosis. LDL modify gene expression in vascular cells leading to disturbances in the functional state of the vessel wall. **Methods:** Expression levels of C-4 sterol methyl oxidase gene (ERG25), sterol regulatory element binding protein (SREBP)-1 and -2 were evaluated in porcine aortic endothelial cells (PAEC), porcine and human smooth muscle cells (SMC) and in the vascular wall from normolipemic and hyperlipemic pigs by RT-PCR. SREBP-1 protein levels were assessed by Western blot and SREBP–SRE binding by EMSA. SREBP-2 was overexpressed by transient transfection with lipofectin. **Results:** We have identified expression of the ERG25 in vascular cells and analyzed its regulation by LDL. ERG25, an enzyme involved in cholesterol biosynthesis, is expressed in vascular endothelial and SMC from porcine and human origin and is downregulated by LDL in a time- and dose-dependent manner. Downregulation of ERG25 by LDL was abolished by an inhibitor of neutral cysteine proteases (*N*-acetyl-leucyl-leucyl-norleucinal) that abrogates SREBP catabolism. LDL downregulated SREBP-2 mRNA levels but not SREBP-1 expression in these cells and both ERG25 and SREBP-2 gene expression was significantly decreased in the vascular wall of diet-induced hypercholesterolemic swine. Finally, in cell transfection experiments SREBP-2 overexpression blocks ERG25 downregulation caused by LDL. **Conclusions:** Our results indicate that LDL modulate ERG25 expression in the vascular wall and suggest the involvement of SREBP-2 in this mechanism.


*Keywords:* Atherosclerosis; Endothelial function; Gene expression; Lipoproteins; Smooth muscle

## 1. Introduction

Plasma LDL levels play a key role in the onset and progression of atherosclerosis [1]. This effect is mediated, at least in part, through the early modulation of gene expression in both endothelial and smooth muscle cells (SMC). In endothelial cells, LDL produce a decrease in nitric oxide bioavailability [2–5] and induce both cell adhesion molecule expression and leukocyte recruitment [6,7] among other effects. In addition, LDL induce mitogenic stimulus in SMC [10], activate SMC expression of proinflammatory factors like TNF-α [11] and transform these cells into foam cells by lipid accumulation [8,9].

The sterol regulatory element binding protein (SREBP) family of transcription factors is involved in the homeostasis of cholesterol and fatty acid metabolism in the liver and adipose tissue [12]. SREBP-2 is the isoform preferentially involved in cholesterol homeostasis while SREBP-1 controls fatty acid metabolism. These transcription factors are synthesized as precursors that remain associated to endoplasmic reticulum and nuclear membranes until sterol levels fall. Then a cascade of proteolytic reactions involving Site-1 and Site-2 proteases, release the mature form that migrates to the nucleus [13–15]. SREBPs regulate transcription of target genes by binding to conserved promoter motifs named sterol regulatory elements (SREs) [13]. We have analyzed the effect of LDL on the expression of both transcription factors and its target genes in vascular cells [5,16–18]. Although expression levels of SREBP-2 were reduced by LDL treatment [5], we have observed that LDL decrease endothelial expression of

*Corresponding author. Tel./fax: +34-93-291-9285.
*E-mail address:* lbmucv@cid.csic.es (L. Badimon).

**Time for primary review 23 days.**

0008-6363/03/$ – see front matter 
doi:10.1016/S0008-6363(02)00856-8

enzymes such as lysyl oxidase [16] and endothelial nitric oxide synthase (eNOS) [5] independently of SREBP-2 downregulation. In this work we have observed for the first time vascular C-4 sterol methyl oxidase (ERG25) expression. This gene involved in a postsqualene phase of cholesterol biosynthesis from 4,4-dimethylzymosterol to zymosterol, is downregulated by LDL both in vitro and in vivo by a SREBP-2-dependent mechanism.

## 2. Methods

### 2.1. Cell culture

Porcine aortic endothelial cells (PAEC) were obtained from adult normolipemic animals as described [16]. Cells were grown in medium M199 (Gibco) supplemented with 10% fetal calf serum (FCS), antibiotics (0.1 mg/ml streptomycin, 100 U/ml penicillin G) and 2 mmol/l L-glutamine. Forty eight hours after plating, cells were placed in 2% FCS medium for 24 h. Then LDL (180 mg cholesterol/dl) were added for another 24 h. Human and porcine SMC were obtained by a modification of the explant technique as described [19,20]. SMC between passages 2 and 6 were grown until subconfluence. Then cells were arrested 48 h in M199 supplemented with 0.2% FCS and incubated with LDL for increasing times. Cell viability was determined by trypan blue exclusion.

### 2.2. Animals

Female pigs (body weight at initiation: 32±4 kg) were randomized into two groups: normolipemic animals ($n=6$) which were fed with a normal chow and hyperlipidemic animals ($n=10$) which were fed with a cholesterol-rich diet (2% cholesterol; 1% cholic acid; 20% beef tallow) for 100 days [21]. Plasma cholesterol levels and hematological parameters were measured at baseline and at sacrifice. Because atherosclerotic lesions develop initially in the abdominal aorta, rings of this vessel were collected and frozen in liquid $N_2$ to measure gene expression. All procedures were in accordance with institutional guidelines and followed the American Physiological Society guidelines for animal research.

### 2.3. Plasma biochemistry

Plasma total cholesterol was determined with an automatic analyzer (Kodak Ektachem DT System). Plasma lipoproteins (HDL-cholesterol, LDL-cholesterol and VLDL-cholesterol) were fractionated using the validated methods of the Lipid Research Clinic Program [22] and quantified spectrophotometrically (Kontron Instruments).

### 2.4. LDL isolation

Porcine or human LDL were obtained from fresh plasma by sequential ultracentrifugation ($d=1.019–1.063$ g/ml). LDL used in the experiments were <72 h old. The purity of LDL was assessed by agarose gel electrophoresis (Paragon System, Beckman). LDL samples had no detectable levels of endotoxin (Limulus Amebocyte Lysate test, Bio Whittaker) and thiobarbituric acid reactive substances values were below 1.5 nmol malonaldehyde/mg protein.

### 2.5. mRNA differential display analysis (mRNA-DD)

Total RNA was isolated using QuickPrep™ total RNA kit (Pharmacia) or Ultraspec™ (Biotecx) according to the manufacturer. mRNA-DD analysis was performed with the Delta™ RNA Fingerprinting kit (Clontech) as described previously [16]. PCR products were loaded on a denaturating 5% polyacrylamide/8 M urea in 0.5× TBE. Bands up- or downregulated by LDL were cut out and DNAs were eluted and reamplified with the same primers used in mRNA-DD. Reamplified products were cloned into the pGEM-T™ easy vector (Promega) and sequenced with the ABIPrism dRhodamine Terminator Cycle Sequencing kit (Perkin Elmer) and the T7 promoter sequencing primer (Promega). Comparison of DNA homology with databases (GenBank) was performed using BLAST.

### 2.6. RT-PCR analysis

ERG25, SREBP-1 and SREBP-2 mRNA levels were analyzed by RT-PCR. One μg of total RNA from control and LDL-treated cells was reverse transcribed [16]. The cDNA obtained was diluted 1:5. An aliquot of 2.5 μl of this dilution was amplified in a 25-μl reaction mixture containing: 2.5 μl PCR DIG labelling Mix (Roche Molecular Biochemicals), 1.3 U Expand™ High Fidelity DNA polymerase (Roche Molecular Biochemicals) and 100 ng of each specific oligonucleotide in 1× buffer and 1.5 mmol/l $MgCl_2$. The specific oligonucleotides selected were: 5′-ggc aag atg ctt tgg ttg tg-3′ (ERG25 upper); 5′-tct cca gaa gca atg tta gc-3′ (ERG25 lower); 5′-tgggaccattctgaccacaa-3′ (SREBP-2 upper); 5′-gccacaggaggagagtctgg-3′ (SREBP-2 lower); 5′-atgtagtcgatggccttgcg-3′ (SREBP-1 upper) and 5′-tgtgacctcgcagatccagc-3′ (SREBP-1 lower). Amplification was carried out by 20 (ERG25), 21 (SREBP-2) or 23 (SREBP-1) cycles of 94 °C 1 min, 61 °C 1 min and 72 °C 2 min followed by a final extension of 72 °C 7 min. Levels of glyceraldehyde-3-phosphate dehydrogenase (GAPDH) were used to normalize results. Detection of digoxigenin (DIG)-labelled nucleic acids was performed as described [16].

### 2.7. Western blot analysis

PAEC were incubated in the presence or in the absence

of LDL (180 mg/dl) for 9 h. Whole-cell extracts (100 μg) were separated by SDS–PAGE (7.5%) and transferred to a nitrocellulose filter (Bio-Rad). Equal loading of protein in each lane was verified by Pounceau staining. Membranes were incubated with a rabbit polyclonal antibody against SREBP-1 (Santa Cruz Biotechnology) used at a dilution of 1:1000.

### 2.8. Electrophoretic mobility shift assay (EMSA)

The double-stranded DNA fragment corresponding to the SRE element present in the SREBP-2 promoter (positions −109 to −128) was used as a probe in EMSA. Nuclear extracts (10 μg) from PAEC were incubated for 15 min on ice with 1 μg of poly[d(I-C)] in 25 mmol/l Tris–HCl (pH 8), 4 mmol/l $MgCl_2$, 5% glycerol, 0.5 mmol/l dithiothreitol, 0.5 mmol/l EDTA and 60 mmol/l KCl (final volume=20 μl). Then, 40,000 cpm of labelled SRE were added and incubation continued for an additional 30 min. DNA–protein complexes were resolved by electrophoresis and were detected by autoradiography.

### 2.9. Transient transfection

PAEC seeded on a six-well plate (180,000 cells/well), were transfected with the SREBP-2–NT expression vector (kindly provided by Dr. Müller-Wieland) that contains the active form of SREBP-2. Transient transfection assays were performed with 1 μg/well of either the SREBP-2–NT plasmid or the empty vector (pcDNA 3; Invitrogen) and 3 μl of lipofectin (Life Technologies). After 5 h of exposure to lipofectin, cells were washed and incubated for 32 h in 1% FCS medium. Then LDL (180 mg/dl) were added for another 7 h and ERG25 mRNA levels were analyzed by RT-PCR.

### 2.10. Statistical analysis

Data are expressed as mean±S.D. (unless stated). Multiple groups were compared by using ANOVA. For the in vivo study statistical differences between groups were analyzed by the Mann–Whitney *U*-test. Differences were considered significant at $P<0.05$.

## 3. Results

### 3.1. ERG25 is expressed in endothelial cells and is downregulated by LDL

PAEC were incubated with atherogenic concentrations of LDL (180 mg/dl) for 24 h and cDNAs from control and LDL-treated cells were compared by mRNA-DD analysis. Twelve combinations of primers T and P were used with cells from different animals and with two dilutions of each cDNA. As shown in Fig. 1A a differential cDNA band was

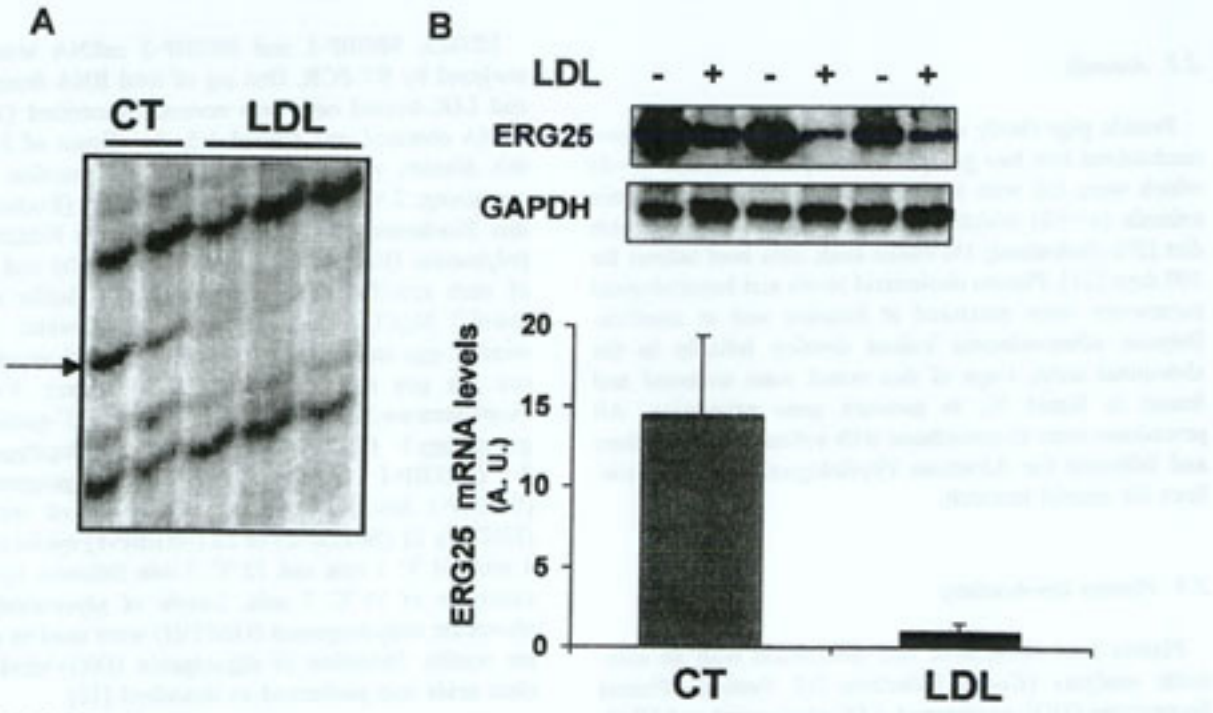


Fig. 1. (A) mRNA-DD analyses were performed with mRNAs from PAEC incubated with LDL (180 mg/dl, 24 h). The arrow shows a band downregulated by LDL treatment. This cDNA was cloned and sequenced showing high homology with human ERG25 (CT, control). (B) mRNA levels of ERG25 and GAPDH were assessed by RT-PCR. A representative blot is shown. Results, normalized by GAPDH mRNA levels ($n=3$), and expressed as media±S.D. (A.U., arbitrary units; $P<0.02$) are shown.

obtained with primers P4 and P7. This cDNA was cloned and sequenced showing high homology (95%) with the human ERG25 gene. Downregulation of ERG25 gene expression by LDL was confirmed by RT-PCR analysis. ERG25 mRNA levels decreased about 14-fold by LDL treatment (1±0.49 vs. controls: 14.3±5) (Fig. 1B). The effect of LDL on ERG25 expression was time- and dose-dependent. The decrease in ERG25 mRNA levels was observed after 4 h of incubation with the highest concentration tested (180 mg/dl) (Fig. 2A). A pronounced reduction was observed even at the smallest concentration assayed after longer incubation times (24 h) (Fig. 2B). ERG25 downregulation by LDL was also observed in SMC from both porcine (Fig. 3) and human origin (data not shown).

### 3.2. SREBP-1 and -2 mRNA levels in vascular cells and in the arterial wall

We analyzed both SREBP-1 and SREBP-2 mRNA levels in PAEC. SREBP-2 mRNA levels were decreased by LDL in a dose- (Fig. 4A) and time-dependent manner (Fig. 4B). By contrast, SREBP-1 mRNA levels (Fig. 4A and B) and protein (Fig. 4C) were unchanged by LDL. Similar results were obtained in SMC from pigs (Fig. 3) and humans (data not shown). Since LDL downregulate ERG25 mRNA levels in both vascular SMC and endothelial cells, we analyzed ERG25 expression in abdominal aorta from normolipemic and hypercholesterolemic animals. The hypercholesterolemic diet increased plasma

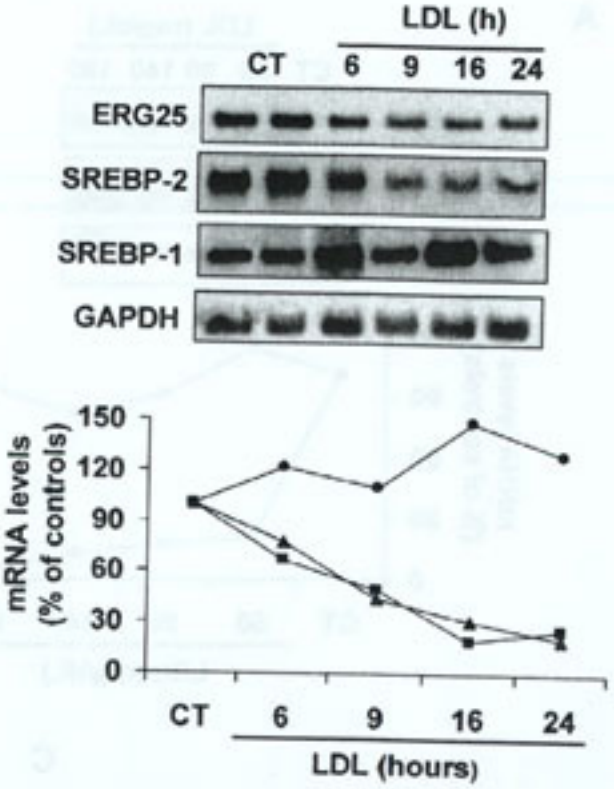


Fig. 3. Time dependence assay performed in pSMC incubated with LDL (150 μg/ml). ERG25 (▲), SREBP-1 (●) and -2 (■) mRNA levels were analyzed by RT-PCR and normalized by GAPDH mRNA levels. Results come from two experiments performed in duplicate.

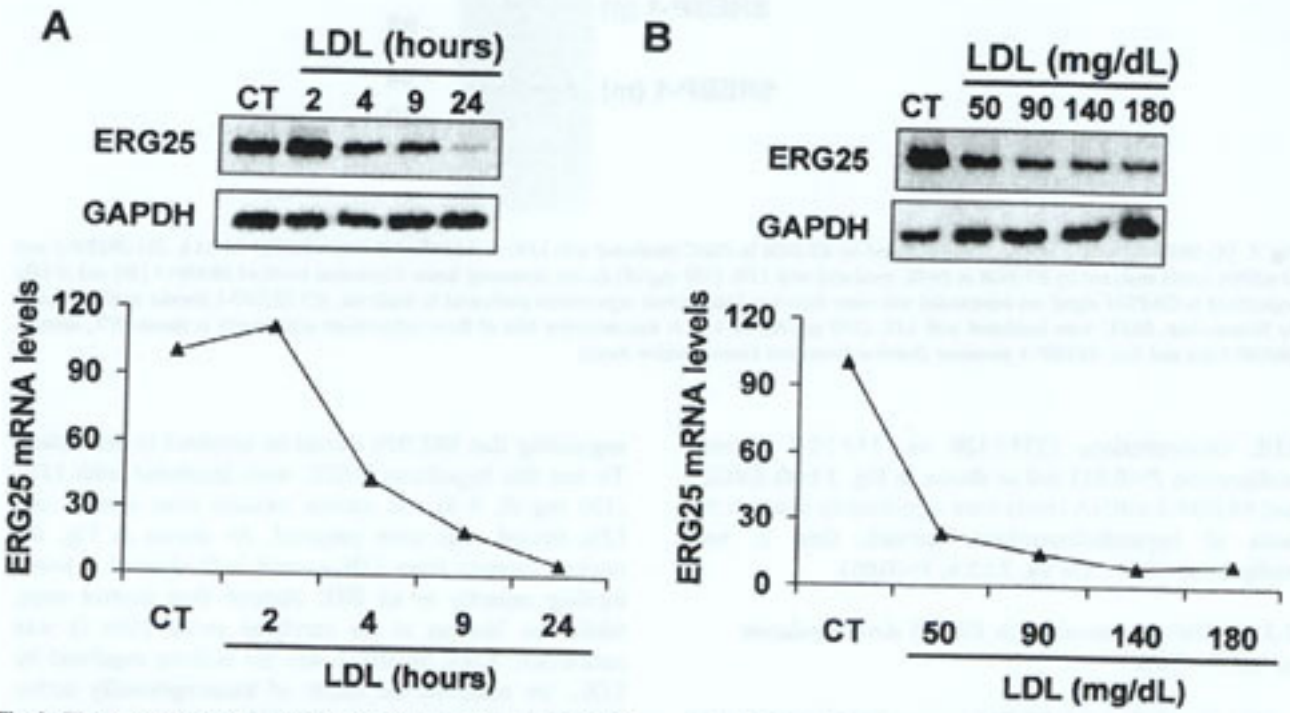


Fig. 2. ERG25 mRNA levels in PAEC. (A) Time-dependence assay: PAEC were incubated with LDL (180 mg/dl) during increasing times and ERG25 mRNA levels were analyzed by RT-PCR. (B) PAEC were incubated with increasing concentrations of LDL during 24 h. GAPDH mRNA levels were used to normalize. Results, from two independent experiments performed in duplicate, are represented graphically as percentage of controls (CT, control).

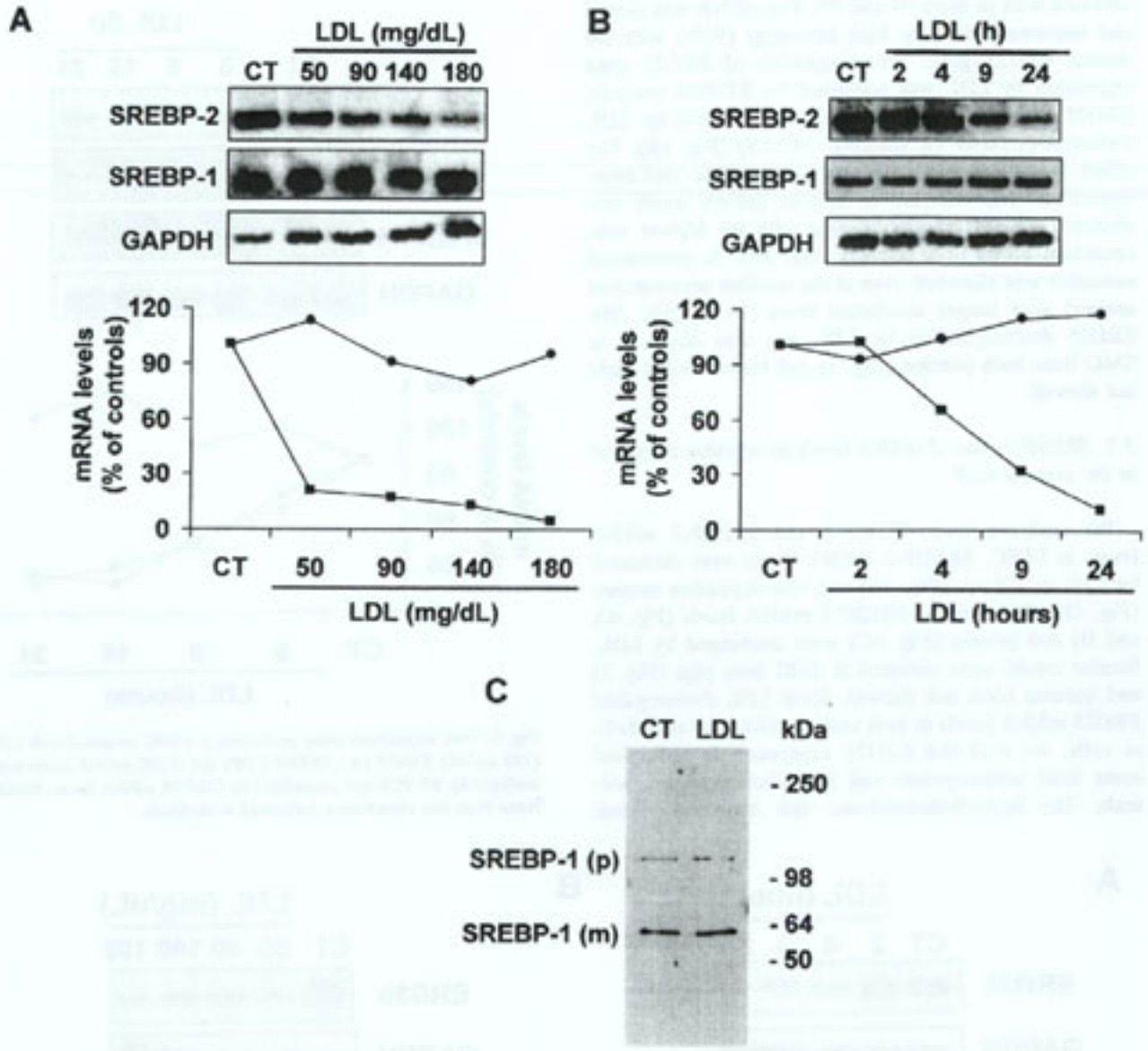


Fig. 4. (A) SREBP-1 and -2 mRNA levels analyzed by RT-PCR in PAEC incubated with LDL at the indicated concentrations for 24 h. (B) SREBP-1 and -2 mRNA levels analyzed by RT-PCR in PAEC incubated with LDL (180 mg/dl) during increasing times. Expression levels of SREBP-1 (●) and -2 (■) normalized to GAPDH signal are represented and come from two independent experiments performed in duplicate. (C) SREBP-1 protein levels analyzed by Western-blot. PAEC were incubated with LDL (180 mg/dl) for 9 h. A representative blot of three independent experiments is shown (CT, control; SREBP-1 (p) and (m), SREBP-1 precursor (inactive form) and mature (active form)).

LDL concentrations (333±120 vs. 34±10.9 in normolipemics; $P<0.01$) and as shown in Fig. 5 both ERG25 and SREBP-2 mRNA levels were significantly lower in the aorta of hypercholesterolemic animals than in normolipemics (2.31±1.6 vs. 7±2.6; $P<0.05$).

### *3.3. SREBP-2 is involved in ERG25 downregulation caused by LDL*

Downregulation of ERG25 expression by LDL was abrogated by ALLN (25 μmol/l), an inhibitor of cysteine proteases that blocks SREBP catabolism (Fig. 6A) [13], suggesting that SREBPs should be involved in this effect. To test this hypothesis, PAEC were incubated with LDL (180 mg/dl, 9 h) and nuclear extracts from control and LDL-treated cells were prepared. As shown in Fig. 6B nuclear extracts from LDL-treated cells showed a lower binding capacity to an SRE element than control ones, while the binding to an unrelated probe (Oct I) was unaffected. Since SREBP-2 was the isoform regulated by LDL, we analyzed the effect of transcriptionally active SREBP-2 overexpression on ERG25 expression. As shown in Fig. 7, the downregulatory effect caused by LDL on ERG25 expression was abrogated in PAEC transfected

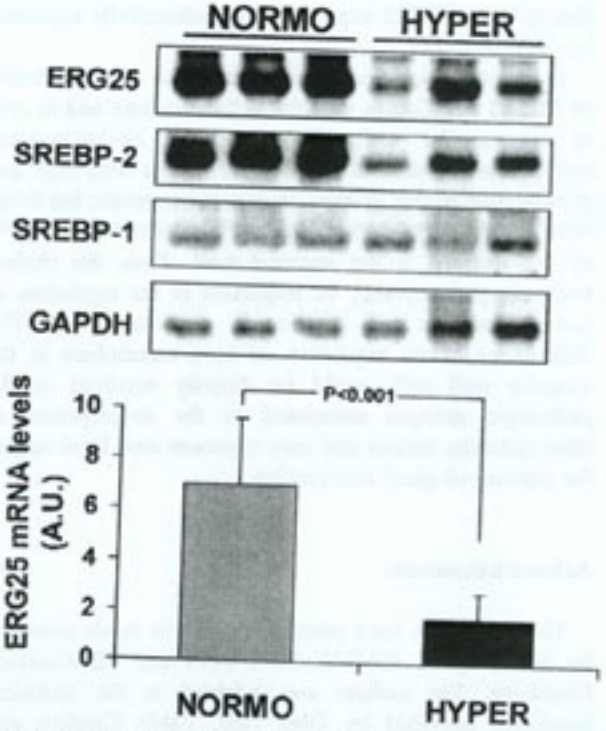


Fig. 5. ERG25, SREBP-1 and -2 mRNA levels were determined by RT-PCR using mRNA from aortic samples of pigs fed with a hypercholesterolemic (HYPER) or with a normolipemic (NORMO) diet. GAPDH was used to normalize results (A.U., arbitrary units).

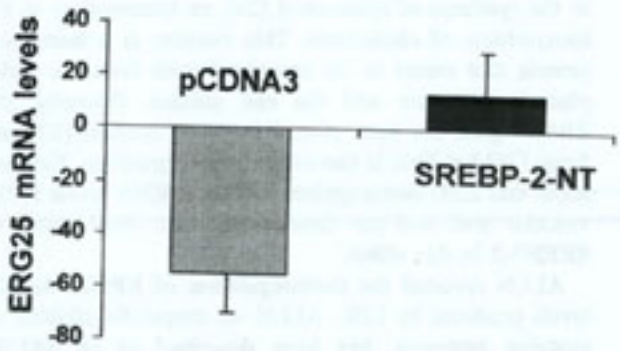


Fig. 7. Effect of LDL (180 mg/dl) on ERG25 mRNA levels from cells transfected with either SREBP-2–NT or pcDNA3. Results are expressed as percent of controls and are the mean±S.E.M. of three experiments performed in duplicate.

with a plasmid (SREBP-2–NT) that expresses the mature form of SREBP-2.

## 4. Discussion

Atherogenic levels of LDL are one of the most important risk factors in atherosclerosis. Hypercholesterolemia induces changes in vascular cell gene expression leading to alterations in vascular function [23–25]. By means of mRNA-DD we have identified for the first time the expression of ERG25 in vascular cells. ERG25 catalyzes the demethylation of 4,4-dimethylzymosterol leading


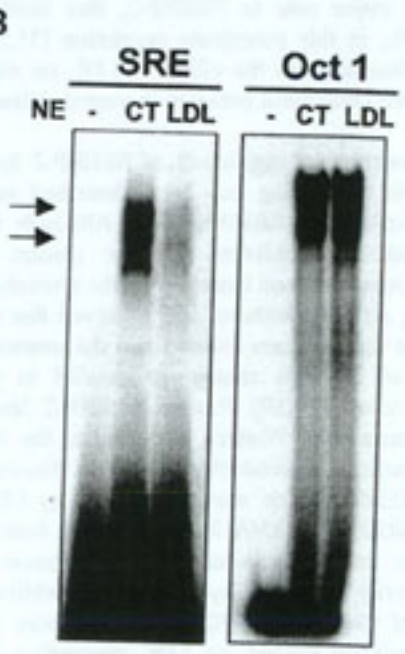


Fig. 6. (A) Representative RT-PCR analysis of ERG25 and GAPDH expression in PAEC incubated with LDL (180 mg/dl) in the presence or absence of ALLN (25 μmol/l, 9 h). GAPDH was used to normalize results. Each assay was performed in duplicate. (B) EMSA assay performed with nuclear extracts from control and LDL-treated cells (9 h, 180 mg/dl) using the SREBP-2–SRE element or the unrelated probe Oct 1. A representative autoradiography of $n=2$ assays is shown.

to the synthesis of zymosterol [26], an intermediary in the biosynthesis of cholesterol. This enzyme is a membrane protein that seems to be associated with both the endoplasmic reticulum and the cell surface. Recently, the ERG25 gene has been cloned in yeast, humans [27] and fungi [28] but little is known about its regulation. Here we show that LDL downregulate ERG25 mRNA levels in the vascular wall and our data suggest the involvement of SREBP-2 in this effect.

ALLN reverted the downregulation of ERG25 mRNA levels produced by LDL. ALLN, an unspecific inhibitor of cysteine proteases, has been described as an SREBP catabolism inhibitor [13,29], thus, SREBPs seem involved in LDL effects. SREBPs regulate several cholesterogenic enzymes in liver, like HMG-CoA reductase, HMG-CoA synthase and farnesyl diphosphate synthase [30–32]. We show that SREBP-2, the isoform involved preferentially in liver cholesterol homeostasis [12], is downregulated by LDL in vascular endothelial and smooth muscle cells. On the contrary, SREBP-1 mRNA levels and both mature and precursor forms of SREBP-1 were not modified by LDL treatment in these cells.

Interestingly, both the ERG25 and SREBP-2 downregulation was also observed in vivo in aortic samples from hypercholesterolemic pigs. Thus, we have observed a parallel regulation of SREBP-2 and ERG25 mRNA levels both in vitro and in the vascular wall. A coordinated regulation of genes encoding enzymes involved in the first steps of cholesterol biosynthesis has been described in different cell types under a variety of conditions including LDL treatment [33,34]. Recent findings in different systems attribute a major role to SREBP-2, that itself is regulated by LDL, in this coordinate regulation [35,36]. However, no information on the effect of LDL on other key enzymes of the cholesterol pathway in vascular tissues is available.

Besides a transcriptional regulation of SREBP-2 itself [37], a proteolytic processing has been described as a regulatory mechanism for SREBPs [14]. Although the proteolytic hypothesis establishes that the content of nuclear SREBPs would depend basically on the proteolytic activity, recently, different authors have observed that the levels of both the nuclear form (active) and the precursor (inactive) form of SREBPs change in parallel to the SREBP mRNA levels [38,39]. Protein SREBP-2 levels could not be measured by Western blot, due to the low efficiency of commercially available antibodies. However, since nuclear SREBP-1 levels were unchanged by LDL, the changes in SREBP-2 mRNA levels observed both in vitro and in vivo may be associated to the decrease in SRE-binding activity observed by EMSA. In addition, overexpression of the active SREBP-2 form blocks the ERG25 downregulation caused by LDL supporting the involvement of this transcription factor in the LDL-mediated effect. Our results are in agreement with recent data from SREBP-1 and SREBP-2 transgenic mice suggesting that in liver ERG25 expression is preferentially regulated by SREBP-2 [40].

In summary, our present data show the downregulation of ERG25 by LDL, in vascular cells in culture and in vivo in the vascular wall. High levels of cholesterogenic enzymes are needed in non-hepatic tissues with high cell growth rates or that synthesize steroid hormones, but it has been surprising to find significant basal expression levels of this enzyme in the vascular wall. Thus, the cholesterogenic pathway may be important in the regulation of cell homeostasis and function in vascular tissues. The disturbance of the regulation of lipid metabolism in the vascular wall cells could be directly involved in the pathologic changes associated to the development of atherosclerotic lesions and may represent new local targets for pharmacological intervention.

## Acknowledgements

This study has been possible thanks to funds provided by MSD, Spain, PN-SAF 2000/0174 and FIC-Catalana Occidente. The authors are indebted to the technical assistance provided by Olga Bell, Pablo Catalina and Silvia Aguiló. B. Raposo and G. Vilahur are predoctoral fellows of CSIC and FIS, respectively.

## References

[1] Fuster V, Badimon L, Badimon JJ, Chesebro JH. The pathogenesis of coronary artery disease and the acute coronary syndromes (part I). N Engl J Med 1992;326:242–250;
Fuster V, Badimon L, Badimon JJ, Chesebro JH. The pathogenesis of coronary artery disease and the acute coronary syndromes (part II). N Engl J Med 1992;326:310–318.

[2] Vidal F, Colomé C, Martínez-González J, Badimon L. Atherogenic concentrations of native low-density lipoproteins down-regulate nitric-oxide-synthase mRNA and protein levels in endothelial cells. Eur J Biochem 1998;252:378–384.

[3] Zhu Y, Liao HL, Wang N et al. Lipoprotein promotes caveolin-1 and ras translocation to caveola: role of cholesterol in endothelial signalling. Arterioscler Thromb Vasc Biol 2000;20:2465–2470.

[4] Boger RH, Sydow K, Borlak J et al. LDL cholesterol upregulates synthesis of asymmetrical dimethylarginine in human endothelial cells: involvement of *S*-adenosylmethionine-dependent methyltransferases. Circ Res 2000;87:99–105.

[5] Martínez-González J, Raposo B, Rodríguez C, Badimon L. HMG-CoA reductase inhibition prevents eNOS downregulation by atherogenic levels of native LDL: balance between transcriptional and post-transcriptional regulation. Arterioscler Thromb Vasc Biol 2001;21:804–809.

[6] Smalley DM, Lin JHC, Curtis ML et al. Native LDL increases endothelial cell adhesiveness by inducing intercellular adhesion molecule-1. Arterioscler Thromb Vasc Biol 1996;16:585–590.

[7] Allen S, Khan S, Al-Mohanna F, Battern P, Yacoub M. Native low density lipoprotein-induced calcium transients trigger VCAM-1 and E-selectin expression in cultured human vascular endothelial cells. J Clin Invest 1998;101:1064–1075.

[8] Campbell JH, Campbell GR. The role of smooth muscle cells in atherosclerosis. Curr Opin Lipidol 1994;5:323–330.

[9] Niemann-Jonsson A, Dimayuga P, Jovinvge S et al. Accumulation of LDL in rat arteries is associated with activation of tumor necrosis factor-alpha expression. Arterioscler Thromb Vasc Biol 2000;20:2205–2211.
[10] Stein O, Stein Y. Smooth muscle cells and atherosclerosis. Curr Opin Lipidol 1995;6:269–274.
[11] Llorente-Cortés V, Martínez-González J, Badimon L. LDL receptor-related protein mediates uptake of aggregated LDL in human vascular smooth muscle cells. Arterioscler Thromb Vasc Biol 2000;20:1572–1579.
[12] Horton JD, Shimomura I. Sterol regulatory element-binding proteins: activators of cholesterol and fatty acid biosynthesis. Curr Opin Lipidol 1999;10:143–150.
[13] Wang X, Sato R, Brown MS, Hua X, Goldstein JL. SREBP-1, a membrane-bound transcription factor released by sterol-regulated proteolysis. Cell 1994;77:53–62.
[14] Brown MS, Goldstein JL. A proteolytic pathway that controls the cholesterol content of membranes, cells and blood. Proc Natl Acad Sci USA 1999;96:11041–11048.
[15] Russell A, Boyd D, Brown MS et al. Transport-dependent proteolysis of SREBP: relocation of site-1 protease from golgi to ER obviates the need for SREBP transport to golgi. Cell 1999;99:703–712.
[16] Rodríguez C, Raposo B, Martínez-González J, Casaní L, Badimon L. Low density lipoprotein downregulate lysyl oxidase in vascular endothelial cells and in the arterial wall. Arterioscler Thromb Vasc Biol 2002;22:1409–1414.
[17] Rodríguez C, Martínez-González J, Sánchez-Gómez S, Badimon L. LDL downregulate CYP51 in porcine vascular endothelial cells and in the arterial wall through a sterol regulatory element binding protein-2-dependent mechanism. Circ Res 2001;88:268–274.
[18] Martínez-González J, Rius J, Badimon L. A nuclear orphan receptor identified in human atherosclerotic plaques is induced by LDL. Atherosclerosis 2000;151:178, Abstract.
[19] Martínez-González J, Badimon L. Human and porcine smooth muscle cells share similar proliferation dependence on the mevalonate pathway: implications for in vivo interventions in the porcine model. Eur J Clin Invest 1996;26:1023–1032.
[20] Llorente-Cortés V, Martínez-González J, Badimon L. Esterified cholesterol accumulation induced by aggregated LDL uptake in human vascular smooth muscle cells is reduced by HMG-CoA reductase inhibitors. Arterioscler Thromb Vasc Biol 1998;18:738–746.
[21] Alfon J, Royo T, García-Moll X, Badimon L. Platelet deposition on eroded vessel wall at stenotic shear rate is inhibited by lipid-lowering treatment with atorvastatin. Arterioscler Thromb Vasc Biol 1999;19:1812–1817.
[22] Lipid Research Clinic Program. Manual of laboratory operation. DHEW publ. no. NIH75-628. Washington, DC: US Government Printing Office, 1974, May.
[23] Li H, Cybulsky MI, Gimbrone MA, Libby P. An atherogenic diet rapidly induces VCAM-1, a cytokine-regulatable mononuclear leukocyte adhesion molecule, in rabbit aortic endothelium. Arterioscler Thromb 1993;13:197–204.
[24] Zeiher AM, Drexler H, Wollschlager H, Just H. Modulation of coronary vasomotor tone in humans. Progressive endothelial dysfunction with different early stages of coronary atherosclerosis. Circulation 1991;83:391–401.
[25] Casino PR, Crescence MK, Quyyumi AA, Hoeg JM, Panza JA. The role of nitric oxide in endothelium-dependent vasodilation of hypercholesterolemic patients. Circulation 1993;88:2541–2547.
[26] Bard M, Bruner DA, Pierson CA et al. Cloning and characterization of ERG25, the *Saccharomyces cerevisiae* gene encoding C-4 sterol methyl oxidase. Proc Natl Acad Sci USA 1996;93:186–190.
[27] Li L, Kaplan J. Characterization of yeast methyl sterol oxidase (ERG25) and identification of a human homologue. J Biol Chem 1996;271:16927–16933.
[28] Kennedy MA, Johnson TA, Lees ND et al. Cloning and sequencing of the *Candida albicans* C-4 sterol methyl oxidase gene (ERG25) and expression of an ERG25 conditional lethal mutation in *Saccharomyces cerevisiae*. Lipids 2000;35:257–262.
[29] Yang J, Sato R, Goldstein JL, Brown MS. Sterol-resistant transcription in CHO cells caused by gene rearrangement that truncates SREBP-2. Genes Dev 1994;8:1910–1919.
[30] Goldstein JL, Brown MS. Regulation of the mevalonate pathway. Nature 1990;343:425–430.
[31] Osborne TF. Transcriptional control mechanisms in the regulation of cholesterol balance. Crit Rev Eukaryot Gene Expr 1995;5:317–335.
[32] Ericsson J, Jackson SM, Lee BC, Edwards PA. Sterol regulatory element binding protein binds to a *cis* element in the promoter of the farnesyl diphosphate synthase gene. Proc Natl Acad Sci USA 1996;93:945–950.
[33] Rossert DS, Ashby MN, Ellist JL, Edwards PA. Coordinate regulation of 3-hydroxy-3-methylglutaryl-coenzyme A synthase, 3-hydroxy-3-methylglutaryl-coenzyme A reductase and prenyltransferase synthesis but not degradation in HepG2 cells. J Biol Chem 1989;264:12653–12656.
[34] Chang TY, Limanek JS. Regulation of cytosolic acetoacetyl coenzyme A thiolase, 3-hydroxy-3-methylglutaryl-coenzyme A synthase, 3-hydroxy-3-methylglutaryl-coenzyme A reductase and mevalonate kinase by low density lipoprotein and by 25-hydroxycholesterol in chinese hamster ovary cells. J Biol Chem 1980;255:7787–7795.
[35] Harris IR, Farrel AM, Holleran WM et al. Parallel regulation of sterol regulatory element binding protein-2 and the enzymes of cholesterol and fatty acid synthesis but not ceramide synthesis in cultured human keratinocytes and murine epidermis. J Lipid Res 1998;39:412–422.
[36] Pai J, Guryev O, Brown MS, Goldstein JL. Differential stimulation of cholesterol and unsaturated fatty acid biosynthesis in cells expressing individual nuclear sterol regulatory element-binding proteins. J Biol Chem 1998;273:26138–26148.
[37] Sato R, Inoue J, Kawabe Y, Kodama T, Takano T, Maeda M. Sterol-dependent transcriptional regulation of sterol regulatory element-binding protein-2. J Biol Chem 1996;271:26461–26464.
[38] Field JF, Born E, Murthy S, Mathur SN. Regulation of sterol regulatory element-binding proteins in hamster intestine by changes in cholesterol flux. J Biol Chem 2001;276:17576–17583.
[39] Kim HJ, Takahashi M, Ezaki O. Fish oil feeding decreases mature sterol regulatory element-binding protein 1 (SREBP-1) by down-regulation of SREBP-1c mRNA in mouse liver. J Biol Chem 1999;274:25892–25898.
[40] Tacer KF, Haugen TB, Baltsen M, Debeljak N, Rozman D. Tissue-specific transcriptional regulation of the cholesterol biosynthetic pathway leads to accumulation of testis meiosis-activating sterol (T-MAS). J Lipid Res 2002;43:82–89.